

Strong regional trends in extreme weather over the next two decades under high- and low-emissions pathways

Article

Accepted Version

Illes, C. E., Samset, B. H., Sandstad, M., Schuhen, N., Wilcox, L. J. ORCID: <https://orcid.org/0000-0001-5691-1493> and Lund, M. T. (2024) Strong regional trends in extreme weather over the next two decades under high- and low-emissions pathways. *Nature Geoscience*, 17. pp. 845-850. ISSN 1752-0908 doi: 10.1038/s41561-024-01511-4 Available at <https://centaur.reading.ac.uk/118570/>

It is advisable to refer to the publisher's version if you intend to cite from the work. See [Guidance on citing](#).

To link to this article DOI: <http://dx.doi.org/10.1038/s41561-024-01511-4>

Publisher: Nature Publishing

All outputs in CentAUR are protected by Intellectual Property Rights law, including copyright law. Copyright and IPR is retained by the creators or other copyright holders. Terms and conditions for use of this material are defined in the [End User Agreement](#).

www.reading.ac.uk/centaur

CentAUR

Central Archive at the University of Reading

Reading's research outputs online

1 **Unprecedented regional trends in extreme weather until 2040, even under**
2 **strong mitigation**

3 Carley E. Iles¹, Bjørn H. Samset¹, Marit Sandstad¹, Nina Schuhen¹, Laura J. Wilcox², Marianne
4 T. Lund¹

5 1. CICERO Center for International Climate Research, Oslo, Norway
6 2. National Centre for Atmospheric Science, Department of Meteorology, University of
7 Reading, Reading, UK

8

9 **Abstract**

10 **Global warming is rapidly shifting climate conditions away from what societies and**
11 **ecosystems are adapted to. While the magnitude of changes in mean and extreme climate**
12 **are broadly studied, regional rates of change, a key driver of climate risk, have received less**
13 **attention. Here we show, using large ensembles of climate model simulations, that large**
14 **parts of the tropics and subtropics, encompassing 70% of current global population, are**
15 **expected to experience unprecedented (>2 standard deviations) joint rates of change in**
16 **temperature and precipitation extremes combined over the next 20 years, under a high**
17 **emissions scenario, dropping to 20% under strong emissions mitigation. This is dominated**
18 **by temperature extremes, with most of the world experiencing unusual (>1 standard**
19 **deviation) rates relative to the pre-industrial, but unusual changes also occur for**
20 **precipitation extremes in northern high latitudes, Southern and Eastern Asia and equatorial**
21 **Africa. However, internal variability is high for 20-year trends, meaning that in the near-**
22 **term, trends of the opposite sign are still likely for precipitation extremes, and rare but not**
23 **impossible for temperature extremes. We also find that rapid clean-up of aerosol emissions,**

24 **mostly over Asia, leads to accelerated co-located increases in warm extremes and influences**
25 **the Asian summer monsoons.**

26

27 Many aspects of the climate are currently entering conditions unprecedented in millennia¹.
28 The present sustained rate of global mean surface warming is also unprecedented in at least
29 the last 2000 years²⁻⁴. Climate risk, and the ability of nature and society to adapt to these new
30 conditions, depend critically on the local rates of change of mean and extreme conditions^{5,6}.
31 Whilst nature and society are accustomed to a certain amount of regional change, due to
32 natural and internal variability of the climate system on various timescales, changes that occur
33 faster than this can be expected to have particularly strong impacts. For instance, rapid
34 changes increase the risk of unprecedented conditions and extreme events such as the record-
35 shattering heatwave in the US Pacific Northwest in 2021, which was deemed impossible
36 without climate change^{7,8}.

37 Extreme events further account for a disproportionate share of the realized impacts of climate
38 change. For instance, heatwaves may cause heat stress and excess mortality of both people
39 and livestock, stress to ecosystems, reduced agricultural yields, difficulties in cooling power
40 plants, and transport disruption. Similarly, precipitation extremes can lead to flooding and
41 damage to settlements, infrastructure, crops and ecosystems, increased erosion and reduced
42 water quality⁹. Thus, society seems particularly vulnerable to high rates of change of extremes,
43 especially when multiple hazards increase at once. There is also an increasing risk of
44 compound events, where extreme conditions occur simultaneously or in succession, which
45 can combine non-linearly to result in greater impacts than would be expected from the sum
46 of each individual component^{10,11}. The 2022 Pakistan floods were likely such an occurrence,

47 where an early heat wave transitioned into an unprecedentedly wet monsoon season. Other
48 examples include combined heat and drought, increasing the risk of wildfires and exacerbating
49 impacts on crops and ecosystems, or the combination of storm surges, caused by strong
50 onshore winds, and heavy inland precipitation, exacerbating coastal flooding^{10,11}. Thus, if a
51 region is projected to experience rapid rates of change in two or more types of extremes, then
52 the rates and intensities of unprecedented compound events may also increase rapidly.

53 Nevertheless, sustained decadal rates of change under global warming remain little studied in
54 comparison to absolute changes, such as average temperatures or changes to the return
55 values of extreme events. For example, the recent IPCC 6th Assessment Report did not
56 systematically assess regional rates of change beyond mean temperatures and precipitation,
57 or include them as a dedicated indicator when quantifying climate risk¹². Also, there is little
58 literature available on how concurrent changes in multiple climate forcers, such as long-lived
59 greenhouse gases and short-lived aerosol emissions, can combine to dampen or amplify
60 regional rates of change on decadal scales.

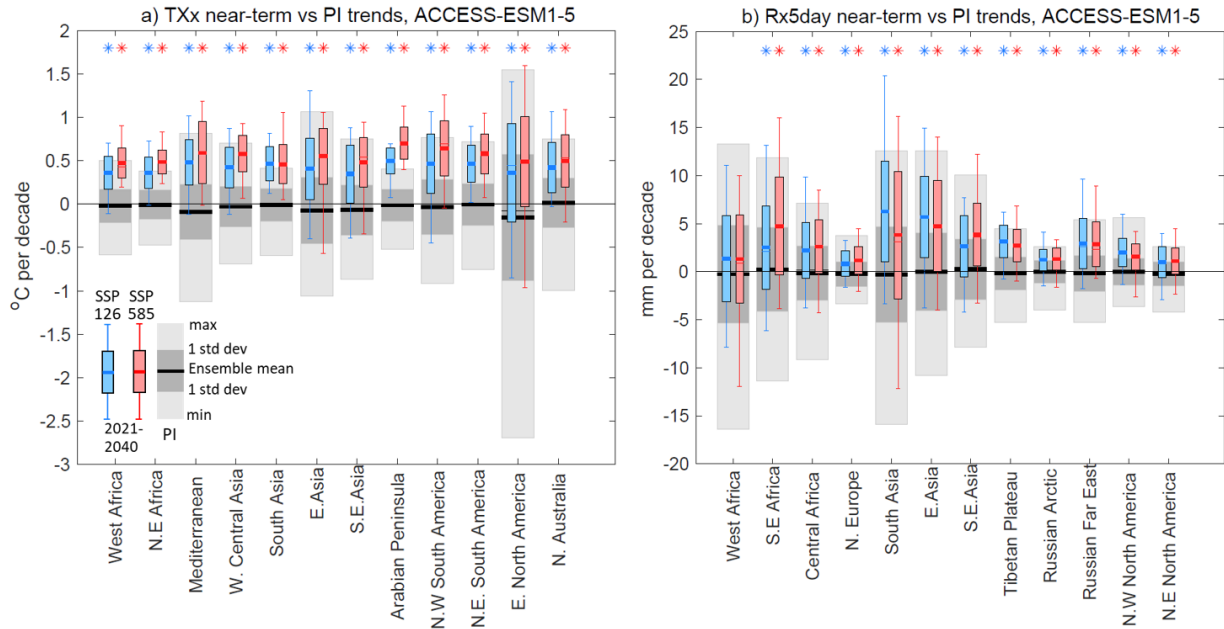
61 Here we examine projected rates of change in temperature and precipitation extremes over
62 the period 2021-2040 ('near-term'), and beyond, compared to pre-industrial rates and
63 variability, using four large ensembles of CMIP6 climate model simulations (ACCESS-ESM1-5,
64 EC-Earth3, CanESM5 and MPI-ESM1-2-LR; see Methods and Table S1). We focus on regional
65 changes, due to their increased relevance to the experience of people and ecosystems
66 compared to the global mean, and identify regions projected to experience substantial
67 changes in rates of one or more extreme event index over the coming decades. The main
68 novelty of our study is to quantify how current forced changes and internal variability interact
69 and play out on a decadal time scale, for a set of commonly used indicators of change.

70 In the following, we first give examples of how near-term regional rates of change of extreme
71 events are projected to accelerate beyond typical pre-industrial variability, even under strong
72 mitigation of greenhouse gas and aerosol emissions, with a focus on areas with strong
73 changes, high population, or both. We then analyse the joint near-term evolution of extreme
74 temperatures and 5-day rainfall events and examine how much of the world's population will
75 experience unprecedented rates in one or both indices^{13–15}. Finally, we discuss how 20-year
76 trends in both indices evolve through to 2080, and the influence of near-term aerosol emission
77 changes on regional rates of change of extreme events.

78

79 **Changes in rates for single extremes indices**

80 In Figure 1, we show near-term (2021-2040) rates of change in the annual maximum of daily
81 maximum temperature (Tx_x), and the amount of precipitation during the wettest 5-day period
82 of the year (Rx5day), compared to the spread of 20-year trends in pre-industrial (PI)
83 conditions. Results shown are from ACCESS-ESM1-5. We use this model for illustration, as it
84 has results that are broadly representative of the multi-model results. ACCESS-ESM1-5 has an
85 Equilibrium Climate Sensitivity (ECS) within the IPCC assessed range (3.9 °C; Methods), and
86 jointly, our four models (shown in the supplement) broadly span the range. This includes a so-
87 called “hot model”, with an ECS of 5.6 °C (CanESM5). We show a selection of IPCC AR6
88 regions¹⁶ where multiple models project clear changes in rates relative to the PI, prioritising
89 those with high present-day population density (see Figure 2) and ensuring representation of
90 all populated continents where we find clear changes (Methods). The remaining regions are
91 shown in Figure S1 and S2.



92

93 **Figure 1: Near-term trends in extremes indices compared to pre-industrial trends.** Trends in
 94 (a) TXx ($^{\circ}\text{C}$ per decade) and (b) Rx5day (mm per decade) for selected AR6 regions for 2021-
 95 2040 compared to 20-year trends in the pre-industrial period, as simulated by the ACCESS-
 96 ESM1-5 40-member large ensemble. For the near-term future, SSP1-2.6 is shown in blue,
 97 SSP5-8.5 in red, whilst the pre-industrial period (PI, defined as 1850-1900) is shown in grey.
 98 Ensemble mean (median) trends are shown with thick (thin) horizontal lines, the standard
 99 deviation spread across members is shown by the boxes for near-term, or dark grey shading
 100 for the pre-industrial, and the entire ensemble spread is shown with the whiskers or light grey
 101 shading respectively. Asterisks indicate whether the difference between PI and near-term
 102 trend distributions are significant based on a K-S test ($p<0.05$). Other models and regions are
 103 shown in Figures S1 and S2.

104

105 For TXx, we find very strong warm shifts in the near-term distribution of 20-year rates of
 106 change, relative to PI, across the ACCESS-ESM1-5 ensemble (K-S test, $p<0.05$, asterisks, see

107 Methods) for all regions in Figure 1a, and for both the high and low emission scenarios. Whilst
108 larger changes relative to the PI can generally be seen in SSP5-8.5 compared to SSP1-2.6,
109 significant changes in rate distributions can be seen in both scenarios and scenario differences
110 are small compared to the overall ensemble spread. The other climate models show a similar
111 overall pattern of results, although CanESM5 tends to show more distinct changes, whilst MPI-
112 ESM1-2-LR shows less distinct changes (Figure S1). These results may reflect their differing
113 climate sensitivities (see Table S1) in agreement with Smith et al., (2015)⁴ and Chavaillaz et al.
114 (2016)¹⁵.

115 Figure 1b shows equivalent results for Rx5day. The regions of clear rapid change in extreme
116 precipitation relative to PI trends tend to include the mid-to high northern latitudes, low
117 latitude Asian and equatorial African countries. Differences in rates of change between the
118 near-term and PI are less clear than for TXx, owing primarily to the higher variability of
119 precipitation. Nevertheless, a significant shift towards wetter extremes is seen for both
120 scenarios in all but one region shown (West Africa), with the near-term ensemble mean rate
121 moving out of the PI standard deviation ensemble spread for at least one scenario (except for
122 Central Africa). Note that the other large ensembles show much clearer changes in rates for
123 West Africa and Central Africa (Figure S2). Scenario differences are also less distinct than for
124 TXx, albeit with hints of stronger differences in regions where the two scenarios differ most
125 strongly in their future aerosol emissions (Supplement). Statistically significant differences in
126 trend distributions in Rx5day between the near-future and PI are also found in many other
127 regions, almost always in a wettening direction (Figure S2).

128 We have also investigated rates of change of consecutive dry days (CDD); see Figures S23-26
129 and S10. Changes in rates are less clear than for TXx or Rx5day compared to pre-industrial

130 trends, although statistically significant changes in trend distributions in CDD do occur in some
131 regions.

132

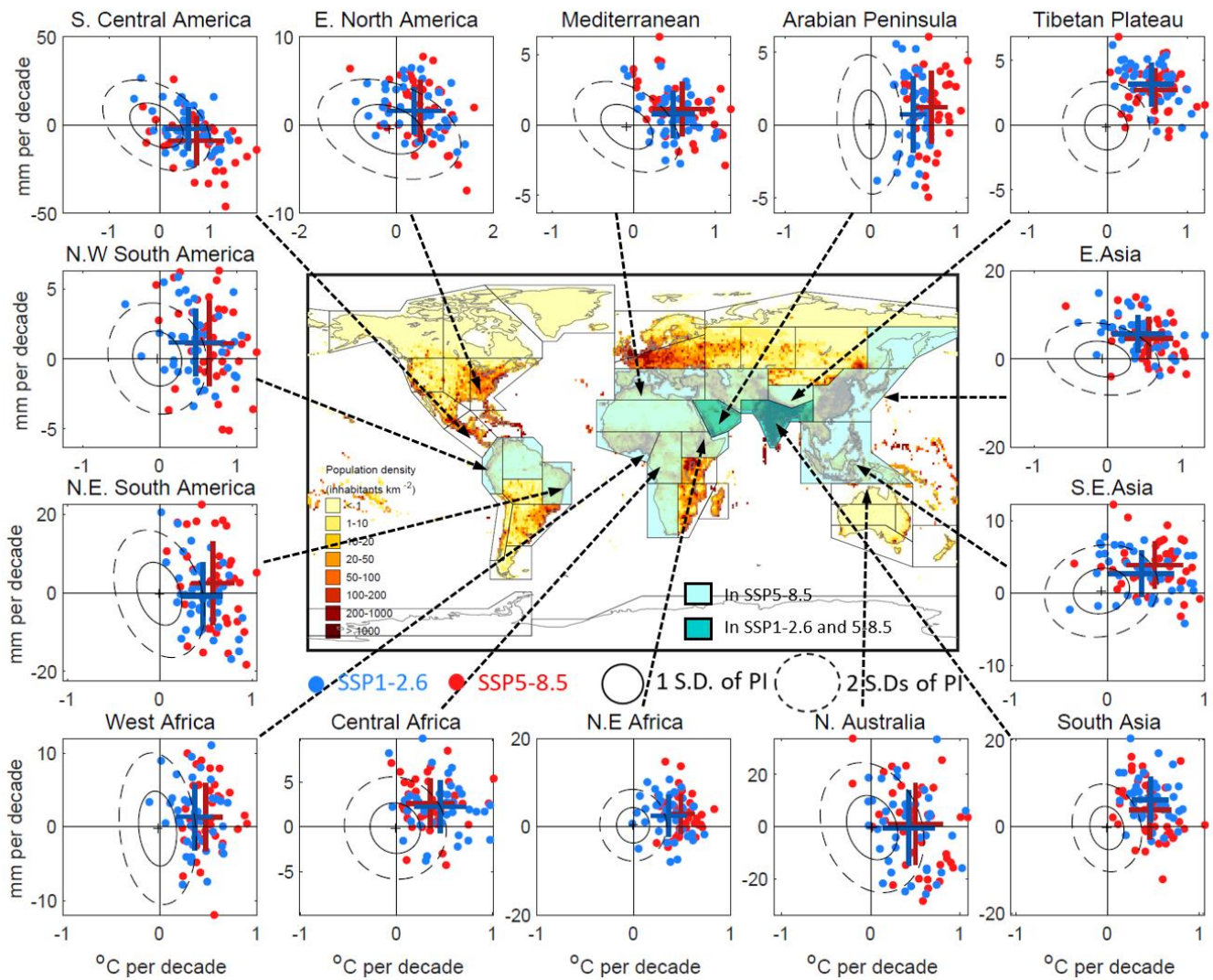
133 **Simultaneous changes in rates for multiple extremes**

134 We now investigate the joint evolution of projected rates of change in both indices. The map
135 in Figure 2 highlights regions undergoing substantial changes in joint rates of change for the
136 near-future relative to the pre-industrial period. Specifically, regions are highlighted that
137 experience a change in ensemble mean joint rates greater than two standard deviations
138 (S.D.s) of pre-industrial trend variability in at least 3 out of 4 models (see Methods). This can
139 be interpreted as a region very likely experiencing sustained, unprecedented rates of change
140 for two or more decades, given that a 2+ standard deviation trend based on large ensembles
141 has a low probability of having occurred over the single realisation of the real world with its
142 limited sample size. Under SSP5-8.5, more than a third of land regions experience joint
143 changes >2 S.D.s for the 2021-2040 period. The regions are clustered at lower latitudes, and
144 often contain low-income countries that are particularly vulnerable to the impacts of climate
145 change, exacerbating the climate risk from this compound hazard. Southern Asia and the
146 Arabian Peninsula are projected to see these unprecedented joint changes also under SSP1-
147 2.6. If we weaken the criterium to one standard deviation of PI variability, almost all regions
148 experience such joint near-term changes under SSP5-8.5, and most also under SSP1-2.6
149 (Figure 3f).

150 The scatterplots in Figure 2 show regional mean near-term rates of changes in TXx vs Rx5day
151 for ACCESS-ESM1-5. To illustrate the influence of internal variability, we include all ensemble
152 members, as well as the ensemble mean and standard deviation spread, and how this

153 compares to the 1 and 2 standard deviation spread of PI rates of change (ellipses, see
154 Methods). The regions shown are those having clear joint changes in the central map,
155 prioritising those with high population, and ensuring at least one region per continent is
156 selected (the rest are shown in Figure S5). In all of these regions, the cloud of points
157 representing the ensemble spread for near-term trends is shifting away from the pre-
158 industrial ellipses¹⁷. Differences between scenarios can be seen, but they are small compared
159 to the size of internal variability. Indeed, trends of the opposite sign to the ensemble means
160 are quite common for some ensemble members for Rx5day over the next 20 years, and cooling
161 trends for TXx are also seen in some members. Broadly consistent results for other models are
162 shown in Figure S6-8.

163



164

165 **Figure 2: Regional joint near-term trends in TXx and Rx5day:** The central map highlights the
 166 regions that show an ensemble mean combined rate of change of TXx and Rx5day for 2021-
 167 2040 that is more than 2 standard deviations of variability in pre-industrial 20-year rates of
 168 change in at least 3 out of 4 models (see Methods) in SSP5-8.5 (light turquoise shading) and
 169 both SSP1-2.6 and 5-8.5 (dark turquoise shading). Population density for 2020 from the
 170 GPWv4 dataset¹⁸ is shown with red shading. Scatterplots show, for selected regions, the trend
 171 in TXx (x-axes) vs Rx5day (y-axes) per decade for 2021-2040 for each ensemble member (dots),
 172 and their ensemble mean trend and standard deviation spread (crosses) for SSP1-2.6 (blue)
 173 and SSP5-8.5 (red) based on the ACCESS-ESM1-5 ensemble. Ellipses show confidence regions

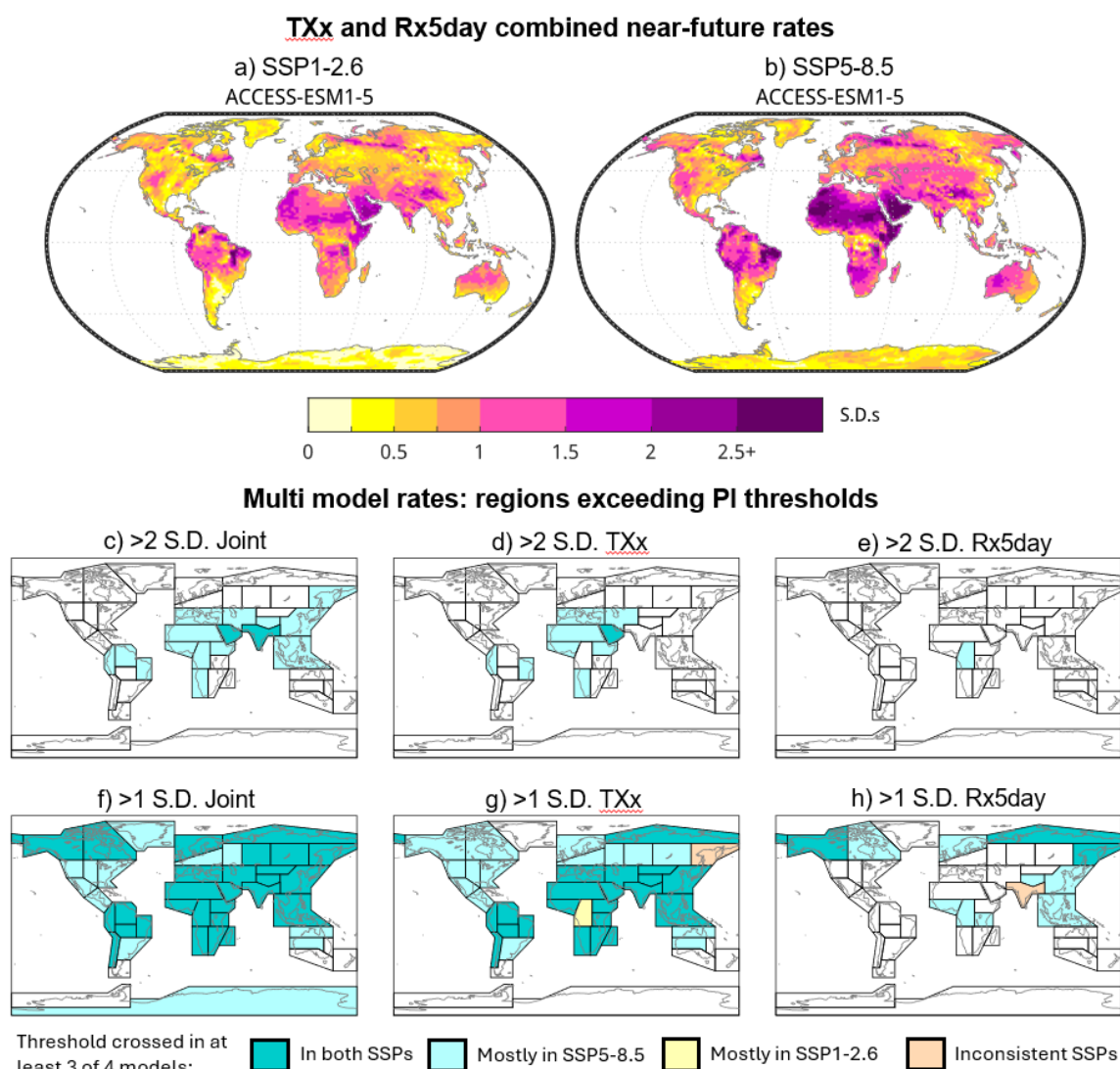
174 for pre-industrial variability of 20-year trends: solid for the 40th percentile confidence ellipse
175 (corresponding to approximately 1 standard deviation) and dashed for 86.5th percentile ellipse
176 (~2 standard deviations, see Methods). The ensemble mean PI trend is indicated with a small
177 black cross.

178

179 Figure 3a-b shows the full spatial patterns of near-term joint TXx and Rx5day rates of change
180 for the ACCESS-ESM1-5 ensemble mean. Combined changes exceed 2 or even 2.5 standard
181 deviations in much of Northern Africa and the Arabian Peninsula, and parts of N.E. South
182 America, Eastern Africa and the Tibetan Plateau under SSP5-8.5. There are also combined
183 rates of change between 1-2 standard deviations over much of northern South America,
184 southern Africa, southern Asia, Western Australia and some parts of North America and
185 Northern Asia. Under SSP1-2.6 changes are more muted but still exceed 1 standard deviation
186 over many low latitude locations. Results are similar for the other models (Figure S9), albeit
187 weaker in MPI-ESM1-2-LR.

188 Figure 3 c-h shows regions with ensemble mean changes in rates exceeding 1 or 2 standard
189 deviations of pre-industrial trend variability in at least 3 of 4 models, for joint changes, and
190 also each index separately. Most land regions experience joint rates of change >1 S.D. in both
191 scenarios, and a large part of the tropics and subtropics experience joint rates >2 S.D.s under
192 SSP5-8.5, but also under SSP1-2.6 for south Asia and the Arabian Peninsula. Almost all regions
193 also experience changes in rates of TXx >1 S.D. in at least one scenario, and parts of Africa,
194 northern South America, Western central Asia, the Arabian Peninsula and southern Europe
195 experience changes >2 S.D.s. These latter are regions with low trend variability (Figure S17)
196 and also correspond well to the regions experiencing the earliest emergence of (absolute)

197 mean and extreme temperature changes from interannual variability^{19–23}. Fewer regions
 198 experience large changes in rates for Rx5day, but nevertheless, changes greater than 1 S.D.
 199 are seen in most high latitude regions in the northern hemisphere, and also in equatorial Africa
 200 and southern and eastern Asia. Central Africa is the only region surpassing 2 S.D.s for Rx5day.
 201 Again, this pattern reflects that of earliest mean and extreme precipitation emergence^{20,24,25}.
 202 Results for individual models can be seen in Figure S4.



203
 204 **Figure 3: Spatial patterns of near-term joint rates of change in extremes, and their**
 205 **components.** Top row: ACCESS-ESM1-5 ensemble mean combined near-term rates of change

206 for TXx and Rx5day expressed in standard deviations of pre-industrial variability of trends, a)
207 for SSP1-2.6, and b) for SSP5-8.5. (c-h) Regions with near-term ensemble mean rates of change
208 greater than 2 (c-e), and 1 (f-h) standard deviations of pre-industrial variability in 20-year
209 trends in at least 3 of 4 models. Panels c and f are for both indices combined (as in Figure 2),
210 whilst d+g is for TXx and e+h for Rx5day. Shading colour indicates which scenario(s) the
211 threshold is crossed in (see Methods for details).

212

213 **Population affected**

214 In Table 1 we show the percentage of global population affected by near-term rates of change
215 larger than 2, 1.5 and 1 standard deviation of pre-industrial variability in 20-year trends, which
216 we define here as unprecedented, highly unusual and unusual respectively. Population
217 affected is taken as the sum of (present-day, land-based) population in regions where 3 or
218 more models show ensemble mean changes in rates passing these thresholds (Methods).

219

% world pop. affected	Joint Changes		TXx		Rx5day	
	ssp126	ssp585	ssp126	ssp585	ssp126	ssp585
>2 S.D.	19.9	68.8	0.9	20.9	0.0	1.7
>1.5 S.D.	59.9	83.3	37.5	72.9	0.0	6.5
>1 S.D.	76.9	90.5	74.5	88.8	19.2	55.9

220
221 **Table 1: Percentage of the world's population affected by strong rates of change of climate
extremes in the next 20 years:** The proportion of global population that will experience near-
222 term (2021-2040) rates of change larger than 2 ("unprecedented"), 1.5 ("highly unusual") and
223 1 ("unusual") standard deviations of pre-industrial variability in 20-year trends, based on the
224 regions highlighted in Figure 3c-h and S3.

226

227 Under SSP5-8.5, almost 70% of the world's current population will experience unprecedented
228 joint rates of change of both indices combined, 83% very unusual and 91% unusual. Even
229 under strong mitigation (SSP1-2.6) 20% of the world's population will experience joint rates
230 larger than 2 S.D.s of PI trends, 60% >1.5 S.D.s, and 77% >1 S.D. A large proportion of
231 population will experience unprecedented (21%), highly unusual (73%) or unusual (89%) rates
232 of change in temperature extremes under SSP5-8.5. This proportion reduces under strong
233 mitigation, but still reaches 38% and 75% for highly unusual and unusual rates of change,
234 respectively. Finally, a smaller proportion of global population will be affected by large
235 changes in rates for precipitation extremes given their higher variability compared to forced
236 changes, but nevertheless 56% of people will experience rates >1 S.D. of pre-industrial rates
237 under SSP5-8.5 and 19% under SSP1-2.6.

238 The reason that more people are affected by large changes in joint rates than might be
239 expected from individual changes in TXx and Rx5day, is that to exceed e.g. 2 S.D.s for joint
240 changes, both individual indices would only need to change by 1.4 S.D.s each (see Methods).
241 When very populous regions, e.g. South Asia or East Asia cross a threshold, this makes a large
242 difference to the population affected.

243

244 **Rates beyond 2040, and the influence of aerosol cleanup**

245 We have also investigated the continued evolution of regional rates of change beyond 2040,
246 and the potential influences of strong near-term reductions in aerosol emissions. Both are
247 shown in detail in the Supplementary Information. As expected, rates of change remain high
248 throughout the 21st century under SSP5-8.5, while they broadly decline in SSP1-2.6 and are

249 largely consistent with preindustrial rates by 2080 (Figures S10-S13). However, even under
250 very strong emissions mitigation and Paris-compatible global warming, we find regions of
251 strong forced rates of change of extreme events until 2060, particularly for warm extremes.
252 Further studies of rates of change, up to and after stabilization of global warming, are
253 therefore warranted. For aerosols, we exploit the fact that over the period 2021-2040, SSP1-
254 2.6 and SSP3-7.0 have only moderately different greenhouse gas concentration trends (Figure
255 S14) but marked differences in aerosol trends, predominantly over Asia. While results are
256 mixed, we do find that aerosol cleanup is associated with an enhanced increase in the warmest
257 days in both summer and winter months over parts of Southern and Eastern Asia,
258 accompanied by a wintertime (DJF) wetting (Figure S15). These results are consistent with the
259 expected influence of a loss of regional, near-source aerosol induced surface cooling. Effects
260 on Asian summer monsoon precipitation were mixed, with two models (ACCESS-ESM1-5 and
261 MPI-ESM1-2-LR) showing statistically significant enhanced monsoon season wet extreme
262 rates.

263 **Discussion**

264 The present analysis is based primarily on large ensembles of climate model simulations,
265 which allow us to explore the role of internal variability, whilst also being able to pin down the
266 models' forced response. This depends, however, on the models being able to realistically
267 simulate decadal rates of change, and their responses to climate forcing. Overall, for the
268 ensemble means we find a robust evolution of both hot and wet extremes across the four
269 models studied, albeit with regional differences consistent with known biases such as
270 monsoon climatologies (Wilcox et al. 2020), and response strengths broadly in line with
271 modelled Equilibrium Climate Sensitivities, particularly for TXx. When looking at individual

realizations there is substantial variability in regional rates of change, even on 20-year timescales, including uncertainty in the sign of the trends. While a lack of pre-industrial observations makes characterizing unprecedented rates of change in climate extremes challenging, large ensembles do indicate how rates of change will likely change between the pre-industrial period and the present day. As our main process of interest here is the internal variability that leads to decadal scale rates of change (and its interactions with forced changes) we have primarily evaluated model performance against this metric (Supplementary Figures S18). Daily precipitation information is unfortunately sparse in many regions, and the short observational record does not allow a large sample of short-term trend periods. However, for TX_x, modelled 20-year trend variability is consistent with observational estimates for the majority of regions. For Rx5day it is well represented in ACCESS-ESM1-5 and CanESM5, especially in the key regions shown in Figures 1-2, but is underestimated in a number of regions in EC-Earth3 and MPI-ESM1-2-LR. Underestimated trend variability may be related to underestimated climatological mean Rx5day, with possible consequences for the size of forced trends (see discussion in supplement), but is unlikely to influence our key results. Assessing whether models are fit-for-purpose for projecting decadal rates of change is clearly a remaining challenge, which cannot be fully resolved with currently available datasets. For the analysis presented here, our overall conclusions of rapid near-term rates of change in major populated regions are generally supported by an agreement between models, observations and reanalysis.

Climate models can also have deficiencies in representing processes such as convective extreme precipitation, which must be parameterized at these resolutions, or mean-state biases. By using four different models we capture some inter-model uncertainty, although this small sample will not fully reflect model uncertainty across CMIP6. The sample of models used

296 include ones that have high climate sensitivities relative to the IPCC likely range (Methods)
297 which may lead to stronger rates for these particular models (see also Smith et al, 2015⁴;
298 Chavaillaz et al., 2016¹⁵) . There is, however, no a priori reason to exclude so-called “hot
299 models” for regional trend analyses, so we do not perform a model selection or weighting of
300 their results here.

301 Whilst over large parts of the globe, these four models agree on the patterns of changes, if
302 not the magnitude, there are regions where Rx5day or CDD are of opposite sign in different
303 models, consistent with greater model uncertainties in projections of precipitation-related
304 quantities than temperature-related ones found in previous studies^{11,26,27}. These differences
305 all constitute uncertainties that should be borne in mind when considering the results of this
306 study.

307 Another caveat is our usage of global, coarse-resolution models, and large geographical
308 regions. These do not capture the full spatial patterns of trends, for which regional, high-
309 resolution modelling would be useful. However, current regional climate models have no, or
310 only rudimentary, treatment of aerosols, and which influences rates-of-change of extreme
311 events both directly and indirectly^{28,29}. Further, the indices used in the present analysis (TXx,
312 Rx5day, CDD) are useful, but not necessarily the most impact relevant in all regions. Further
313 work is critically needed on regional rates-of-change of extremes using updated regional
314 models, and locally adapted, multi-hazard indicators.

315 We find that over the coming decades, regional trends in extreme weather well beyond
316 internal variability are likely in many regions, affecting a large fraction of global population,
317 even under strong emissions mitigation. These conclusions emphasize the need for both

318 continued mitigation and adaptation to potentially unprecedented changes over the next 20
319 years even under a low emissions scenario.

320

321 **Corresponding author**

322 Correspondence should be addressed to Carley Iles: carley.iles@cicero.oslo.no

323

324 **Acknowledgements**

325 This research has received funding from the European Union's Horizon 2020 research and
326 innovation programme under grant agreements No 101003826 through the CRiceS project
327 and No 820655 through the EXHAUSTION project and also from the Norwegian Research
328 Council through the projects CATHY (324182) and QUISARC (248834). We acknowledge the
329 Centre for Advanced Study in Oslo, Norway that funded and hosted our HETCLIF centre during
330 the academic year of 2023/24. We acknowledge the World Climate Research Programme,
331 which, through its Working Group on Coupled Modelling, coordinated and promoted CMIP6.
332 We thank the climate modelling groups for producing and making available their model
333 output, the Earth System Grid Federation (ESGF) for archiving the data and providing access,
334 and the multiple funding agencies who support CMIP6 and ESGF.

335

336 **Author Contributions**

337 CI and BHS conceived and designed the experiments, CI performed the experiments and
338 analysed the data, MS contributed materials/analysis tools, all authors wrote the paper.

340 **References**

- 341 1. IPCC. Summary for Policymakers. in *Climate Change 2021: The Physical Science Basis. Contribution of Working Group I to the Sixth Assessment Report of the Intergovernmental Panel on Climate Change* (eds. Masson-Delmotte, V. et al.) 3–32 (Cambridge University Press, 2021). doi:10.1017/9781009157896.001.
- 342 2. Gulev, S. K. *et al.* Changing State of the Climate System. in *Climate Change 2021: The Physical Science Basis. Contribution of Working Group I to the Sixth Assessment Report of the Intergovernmental Panel on Climate Change* (eds. Masson-Delmotte, V. et al.) 287–422 (Cambridge University Press, 2021). doi:10.1017/9781009157896.004.
- 343 3. Samset, B. H. *et al.* Steady global surface warming from 1973 to 2022 but increased warming rate after 1990. *Commun. Earth Environ.* **4**, 400 (2023).
- 344 4. Smith, S. J., Edmonds, J., Hartin, C. A., Mundra, A. & Calvin, K. Near-term acceleration in the rate of temperature change. *Nat. Clim. Chang.* **5**, 333–336 (2015).
- 345 5. Loarie, S. R. *et al.* The velocity of climate change. *Nature* **462**, 1052–1055 (2009).
- 346 6. O'Neill, B. C. & Oppenheimer, M. Climate change impacts are sensitive to the concentration stabilization path. *Proc. Natl. Acad. Sci.* **101**, 16411–16416 (2004).
- 347 7. Fischer, E. M., Sippel, S. & Knutti, R. Increasing probability of record-shattering climate extremes. *Nat. Clim. Chang.* **11**, 689–695 (2021).
- 348 8. Philip, S. Y. *et al.* Rapid attribution analysis of the extraordinary heat wave on the Pacific coast of the US and Canada in June 2021. *Earth Syst. Dyn.* **13**, 1689–1713

- 360 (2022).
- 361 9. Ranasinghe, R. *et al.* Climate Change Information for Regional Impact and for Risk
362 Assessment. in *Climate Change 2021: The Physical Science Basis. Contribution of*
363 *Working Group I to the Sixth Assessment Report of the Intergovernmental Panel on*
364 *Climate Change* (eds. Masson-Delmotte, V. *et al.*) 1767–1926 (Cambridge University
365 Press, 2021). doi:10.1017/9781009157896.014.
- 366 10. Zscheischler, J. *et al.* Future climate risk from compound events. *Nat. Clim. Chang.* **8**,
367 469–477 (2018).
- 368 11. Seneviratne, S. I. *et al.* Weather and Climate Extreme Events in a Changing Climate. in
369 *Climate Change 2021: The Physical Science Basis. Contribution of Working Group I to*
370 *the Sixth Assessment Report of the Intergovernmental Panel on Climate Change* (eds.
371 Masson-Delmotte, V. *et al.*) 1513–1766 (Cambridge University Press, 2021).
372 doi:10.1017/9781009157896.013.
- 373 12. IPCC. *Climate Change 2021: The Physical Science Basis. Contribution of Working Group*
374 *I to the Sixth Assessment Report of the Intergovernmental Panel on Climate Change.*
375 (Cambridge University Press, 2021). doi:10.1017/9781009157896.
- 376 13. Sedláček, J. & Knutti, R. Half of the world’s population experience robust changes in
377 the water cycle for a 2 °C warmer world. *Environ. Res. Lett.* **9**, 044008 (2014).
- 378 14. Lehner, F. & Stocker, T. F. From local perception to global perspective. *Nat. Clim.*
379 *Chang.* **5**, 731–734 (2015).
- 380 15. Chavaillaz, Y., Joussaume, S., Dehecq, A., Braconnot, P. & Vautard, R. Investigating the
381 pace of temperature change and its implications over the twenty-first century. *Clim.*

- 404 23. Mahlstein, I., Knutti, R., Solomon, S. & Portmann, R. W. Early onset of significant local
405 warming in low latitude countries. *Environ. Res. Lett.* **6**, 034009 (2011).
- 406 24. Nguyen, T.-H., Min, S.-K., Paik, S. & Lee, D. Time of emergence in regional precipitation
407 changes: an updated assessment using the CMIP5 multi-model ensemble. *Clim. Dyn.*
408 **51**, 3179–3193 (2018).
- 409 25. Mahlstein, I., Portmann, R. W., Daniel, J. S., Solomon, S. & Knutti, R. Perceptible
410 changes in regional precipitation in a future climate. *Geophys. Res. Lett.* **39**, (2012).
- 411 26. Hawkins, E. & Sutton, R. The potential to narrow uncertainty in projections of regional
412 precipitation change. *Clim. Dyn.* **37**, 407–418 (2011).
- 413 27. Lehner, F. *et al.* Partitioning climate projection uncertainty with multiple large
414 ensembles and CMIP5/6. *Earth Syst. Dyn.* **11**, 491–508 (2020).
- 415 28. Persad, G. *et al.* Rapidly evolving aerosol emissions are a dangerous omission from
416 near-term climate risk assessments. *Environ. Res. Clim.* **2**, 032001 (2023).
- 417 29. Schumacher, D. L. *et al.* Exacerbated summer European warming not captured by
418 climate models neglecting long-term aerosol changes. *Commun. Earth Environ.* **5**, 182
419 (2024).
- 420
- 421
- 422

423 **Online Methods**

424 **Climate model simulations**

425 We analyse four large ensembles of climate model simulations produced as part of the CMIP6
426 exercise³⁰: ACCESS-ESM1-5 (40 members³¹), MPI-ESM1-2-LR (30³²), CanESM5 (50³³) and EC-
427 Earth3 (57; 20 for the preindustrial case^{34,35}). See Table S1 for details. The equilibrium climate
428 sensitivities (ECS) of these models range from the IPCC AR6 best estimate (MPI-ESM1-2-LR;
429 3.0°C for a doubling of CO₂ concentrations), to a value at the upper end of the CMIP6 range
430 (CanESM5; 5.6°C)^{1,36}. ACCESS-ESM1-5 has an ECS of 3.9°C, EC-Earth3 has 4.3°C. The IPCC likely
431 range is 2.5-4°C and very likely range 2-5°C.

432 We use the historical CMIP6 simulations for the pre-industrial period, and the future scenarios
433 SSP1-2.6, SSP5-8.5 and SSP3-7.0. The historical simulations are forced with observed records
434 of both anthropogenic and natural forcing agents, including greenhouse gases, anthropogenic
435 aerosols, volcanic aerosols, solar variability and land-use change³⁰. The future scenarios
436 include various possible trajectories of greenhouse gas emissions, land use and aerosols³⁷. To
437 assess the influence of emissions trajectories on trends over the coming 20 years, we contrast
438 a very low (SSP1-2.6) and very high (SSP5-8.5) greenhouse gas emissions scenario. When
439 examining trends related to aerosol clean-up, we contrast SSP1-2.6 with SSP3-7.0, the former
440 having rapid aerosol reductions over the next 20 years, notably from India and China, and the
441 latter having continued growth of emissions (see Figure S14).

442 We use ACCESS-ESM1-5 as an example model in the main text, since it has a climate sensitivity
443 consistent with recent assessments, and middle of the range results compared to the other
444 models, as well as reasonable trend variability compared to ERA5 (Supplementary Material).

445 The other models are fully presented in the supplement. Multi-model results are based on all
446 four models, as described below.

447 **Extreme event indices**

448 We analyse regional trends in two widely used climate extremes indices that form part of the
449 Expert Team on Climate Change Detection and Indices (ETCCDI) set of indices³⁸: The annual
450 maximum of daily maximum temperatures (TXx), as a measure of heat extremes, and the total
451 precipitation falling in the wettest 5 consecutive day period of the year (Rx5day) as a measure
452 of wet extremes. We also present further analysis for dry extremes in the supplement, for the
453 maximum number of consecutive dry days per year (CDD). We use a version where the dry
454 spell is not allowed to continue past the year boundary, i.e. the maximum value is 365 days
455 per year.

456 **Near-term and preindustrial trends**

457 We calculate trends over the period 2021-2040, defined here as the “near-term”, using a
458 linear regression of yearly ETCCDI index values for each model ensemble member. For regional
459 results we calculate the regional-mean land-only time series first and then calculate trends,
460 whilst for spatial plots trends are calculated per grid cell. We also calculate 20-year trends for
461 the preindustrial (PI) period by examining 20-year periods within the time frame 1850-1900,
462 shifting the start year by 5 years each time. This yields a total sample size of 7x 20-year trends
463 per ensemble member. This method was chosen to avoid trends driven by the effect of
464 volcanic eruptions overly influencing the PI trends (see Figure S16).

465 **Combined rates of change**

466 As well as near-term rates of change for the separate extreme indices, we examine joint rates
467 of change in TXx and Rx5day, to identify regions subject to multiple stressors at the same time.

468 In order to relate changes to preindustrial variability of 20-year trends, we convert changes in
469 both indices to units of standard deviations of their PI trend variability. We then define a
470 combined trend as the sum of squares of the two metric trends:

$$471 \quad \text{Combined trend} = \sqrt{\left(\frac{R_{TXx}^{\text{near-term}} - R_{TXx}^{\text{PI}}}{\sigma(r_{TXx}^{\text{PI}})} \right)^2 + \left(\frac{R_{Rx5day}^{\text{near-term}} - R_{Rx5day}^{\text{PI}}}{\sigma(r_{Rx5day}^{\text{PI}})} \right)^2}$$

472 Here, r_x^y is the 20-year rate-of-change in a single ensemble member, for indicator x in period
473 y (near-term future or preindustrial (PI)), R_x^y is the corresponding ensemble mean, and σ is the
474 standard deviation across all ensemble members.

475 As an example, if both indices exhibit an increase in the ensemble mean rate of change
476 between the near-term and PI that is 1 standard deviation of the PI variability of trends, then
477 the combined trend will be 1.4.

478 **Evaluation against observational datasets**

479 To assess the representation of 20-year trend variability in the climate models used for this
480 study, we perform a regional comparison with the ERA5 reanalysis³⁹ for TXx and Rx5day, and
481 additionally the Rainfall Estimates on a Gridded Network (REGEN) daily gauge-based dataset
482 for Rx5day⁴⁰. ERA5 temperature and precipitation data were available for the period 1941-
483 2022 on a 0.25°grid, whilst REGEN is available from 1950-2016 on a 1°grid. REGEN combines
484 stations from the Global Precipitation Climatology Centre (GPCC)⁴¹, Global Historical
485 Climatology Network – Daily (GHCN-daily)⁴² and other sources, and is available as two
486 versions: REGEN-LONG, which includes only stations with at least 40 years of data, and REGEN-

487 ALL, which includes a much larger number of stations. Each is spatially interpolated and comes
488 with a data quality mask. TXx and Rx5day were calculated in the same way as for the climate
489 model data. The results of the evaluation are presented in the Supplementary Materials
490 (Figures S18).

491 **Region selection**

492 We calculate regional results for the 46 land regions defined as part of the IPCC sixth
493 assessment cycle¹⁶, with a further masking applied to retain only grid cells with >50% land.
494 These regions are widely used for climate studies and are a refined version of those used in
495 previous IPCC cycles. They are defined with climate homogeneity in mind, both in terms of
496 historical mean climate and projections, whilst also being large enough to be appropriate for
497 use with the CMIP6 generation of models, at around 1 degree resolution.

498 Where a sub-selection of regions is shown, e.g. in Figures 1 and 2, these are subjectively
499 chosen based on a combination of 1) showing a clear shift in the distribution of trends away
500 from the pre-industrial equivalent, 2) prioritising regions with high population density and 3)
501 representing all continents where we find clear changes. More specifically, for combined rates
502 of change, and for TXx point 1) is based on regions undergoing an ensemble mean rate at least
503 1.5 standard deviations bigger than the PI equivalent in at least three models (as seen in
504 Figures 3 and S3), whilst for Rx5day, where changes are less clear relative to PI due to higher
505 intrinsic variability, we use a lower threshold of 1 standard deviation. Results for remaining
506 regions are shown in the supplement.

507 **Colour coding of SSPs in multi-model regional map figures**

508 In Figures 2, 3, S3 and S4, regions are colour coded according to the SSP in which a given
509 threshold is crossed. The thresholds are defined as when the change in ensemble mean rates

510 between the PI and near-term is greater than the PI 20-year trend variability by a certain
511 number of standard deviations.

512 Two SSPs are examined (SSP1-2.6 and SSP5-8.5). For single model plots there are thus four
513 options for threshold crossing: In either SSP5-8.5, or SSP1-2.6, or both, or none. For the multi
514 model plots, we use the following colour coding:

515 1) The given threshold must be passed in at least 3 of 4 models for a colour to be assigned.

516

517 2) The colour categories are then as follows:

518 - “In both SSPs” (teal)- at least 3 models cross the threshold for both SSPs (this includes
519 situations where 3 models cross the threshold in both SSPs, and the last model crosses
520 for only one SSP)

521 - “Mostly in SSP5-8.5” (light cyan)- More models cross the threshold for SSP5-8.5 than
522 for SSP1-2.6

523 - “Mostly in SSP1-2.6” (yellow)- More models cross the threshold for SSP1-2.6 than for
524 SSP5-8.5

525 - Inconsistent SSPs (orange)- any combination that does not fit into the previous
526 categories e.g. two models only cross the threshold in SSP5-8.5 and the other two only
527 for SSP1-2.6, or 1 model only SSP5-8.5, another only SSP1-2.6 and the remaining two
528 both SSPs.

529 **Population calculations**

530 Population density and totals for the year 2020 are taken from the United Nations World
531 Population Prospects Gridded Population of the World, Adjusted Version 4 dataset, on a 1
532 degree grid^{18,43}. Whilst population will change over the next 20 years, some of the regions

533 with the clearest acceleration in rates of change are also those where population is projected
534 to increase fastest e.g. Africa, likely putting our results on the conservative side. When
535 calculating the percentage of the global population affected by near-term rates of change in
536 extreme indices greater than a given threshold of preindustrial variability of 20-year trends,
537 we sum up the populations in the AR6 WG1 regions affected by such changes as shown in
538 Figure 3c-f and S3. These are regions where 3 out of 4 large ensembles show ensemble mean
539 changes in rates passing these thresholds. For SSP5-8.5 estimates we include teal, light cyan
540 and orange regions (i.e. threshold is crossed mostly in SSP5-8.5, both SSPs and inconsistent
541 SSPs respectively- see previous section), and for SSP1-2-6 teal, yellow and orange regions
542 (both SSPs, mostly SSP1-2.6 and inconsistent SSPs respectively).

543 Since the climate data are masked to land only, we also mask population data to land only
544 when calculating the total population affected. This means that 90.8% of the world's
545 population is considered in our analysis. Population affected is then expressed as a percentage
546 of total global unmasked population. This means that our population affected estimates are
547 on the conservative side, since we cannot say anything about the remaining population, for
548 example in some small islands.

549 **Statistical Testing**

550 We use a two-sample Kolmogorov Smirnov test (K-S test) to test whether the differences
551 between empirical distributions of 20-year trends between two periods or two scenarios from
552 a given climate model ensemble are statistically significant at the 5% significance level. The K-
553 S test is a non-parametric test which compares two samples and tries to determine whether
554 these come from the same underlying continuous distribution by examining the maximum
555 distance between the empirical distribution functions based on the two samples. For this test,

556 the underlying distribution does not have to be specified or even known and it takes both
557 location and shape of the distribution into account.

558 **Ellipses**

559 The ellipses shown in Figures 2, S5-8 and S19-22 correspond to the area covered by the 40th
560 and 86.5th percentiles of the bivariate distributions of the 20-year trends in TXx vs Rx5day for
561 the preindustrial period, estimated from their respective covariance matrices. This
562 corresponds approximately to one and two standard deviations, respectively, of the chi-
563 squared distribution generated from the sum of the squared components of the bivariate
564 distribution.

565

566

567 **Data availability**

568 The climate model data used for this analysis are publicly available from the ESGF portals
569 e.g. <https://esgf-data.dkrz.de/search/cmip6-dkrz/>. ETCCDI indices for CMIP6 models are
570 available from the Copernicus Climate Data Store at
571 [https://cds.climate.copernicus.eu/cdsapp#!/dataset/sis-extreme-indices-
572 cmip6?tab=overview](https://cds.climate.copernicus.eu/cdsapp#!/dataset/sis-extreme-indices-cmip6?tab=overview). ERA5 temperature and precipitation data are available from
573 [https://cds.climate.copernicus.eu/cdsapp#!/dataset/reanalysis-era5-single-
575 levels?tab=overview](https://cds.climate.copernicus.eu/cdsapp#!/dataset/reanalysis-era5-single-
574 levels?tab=overview). REGEN-LONG is available from <https://zenodo.org/records/4922162>
576 and REGEN-ALL from <https://zenodo.org/records/4922160>. Population data are available
from <https://sedac.ciesin.columbia.edu/data/collection/gpw-v4>.

577

578 **Code availability**

579 The code used in this analysis will be deposited in a publicly accessible archive and made
580 available upon publication of this manuscript.

581 **Methods References**

582 30. Eyring, V. *et al.* Overview of the Coupled Model Intercomparison Project Phase 6
583 (CMIP6) experimental design and organization. *Geosci. Model Dev.* **9**, 1937–1958
584 (2016).

585 31. Mackallah, C. *et al.* ACCESS datasets for CMIP6: methodology and idealised
586 experiments. *J. South. Hemisph. Earth Syst. Sci.* **72**, 93–116 (2022).

587 32. Mauritsen, T. *et al.* Developments in the MPI-M Earth System Model version 1.2 (MPI-
588 ESM1.2) and Its Response to Increasing CO₂. *J. Adv. Model. Earth Syst.* **11**, 998–1038
589 (2019).

590 33. Swart, N. C. *et al.* CCCma CanESM5 model output prepared for CMIP6 CMIP historical.
591 (2019) doi:10.22033/ESGF/CMIP6.3610.

592 34. Döscher, R. *et al.* The EC-Earth3 Earth system model for the Coupled Model
593 Intercomparison Project 6. *Geosci. Model Dev.* **15**, 2973–3020 (2022).

594 35. Wyser, K. *et al.* The SMHI Large Ensemble (SMHI-LENS) with EC-Earth3.3.1. *Geosci.*
595 *Model Dev.* **14**, 4781–4796 (2021).

596 36. Meehl, G. A. *et al.* Context for interpreting equilibrium climate sensitivity and
597 transient climate response from the CMIP6 Earth system models. *Sci. Adv.* **6**,
598 eaba1981 (2022).

- 599 37. O'Neill, B. C. *et al.* The Scenario Model Intercomparison Project (ScenarioMIP) for
600 CMIP6. *Geosci. Model Dev.* **9**, 3461–3482 (2016).
- 601 38. Sillmann, J., Kharin, V. V., Zhang, X., Zwiers, F. W. & Bronaugh, D. Climate extremes
602 indices in the CMIP5 multimodel ensemble: Part 1. Model evaluation in the present
603 climate. *J. Geophys. Res. Atmos.* **118**, 1716–1733 (2013).
- 604 39. Hersbach, H. *et al.* The ERA5 global reanalysis. *Q. J. R. Meteorol. Soc.* **146**, 1999–2049
605 (2020).
- 606 40. Contractor, S. *et al.* Rainfall Estimates on a Gridded Network (REGEN) – a global land-
607 based gridded dataset of daily precipitation from 1950 to 2016. *Hydrol. Earth Syst. Sci.*
608 **24**, 919–943 (2020).
- 609 41. Ziese, M. *et al.* GPCC Full Data Daily Version.2018 at 1.0°: Daily Land-Surface
610 Precipitation from Rain-Gauges built on GTS-based and Historic Data. (2018)
611 doi:10.5676/DWD_GPCC/FD_D_V2018_100.
- 612 42. Menne, M. J., Durre, I., Vose, R. S., Gleason, B. E. & Houston, T. G. An Overview of the
613 Global Historical Climatology Network-Daily Database. *J. Atmos. Ocean. Technol.* **29**,
614 897–910 (2012).
- 615 43. Center for International Earth Science Information Network-CIESIN-Columbia
616 University. Gridded Population of the World, Version 4 (GPWv4): Population Count
617 Adjusted to Match 2015 Revision of UN WPP Country Totals, Revision 11. (2018)
618 doi:<https://doi.org/10.7927/H4PN93PB>.
- 619